Electrochimica Acta 53 (2008) 7248–7254

Contents lists available at ScienceDirect

Electrochimica Acta

journal homepage: www.elsevier.com/locate/electacta

Evaluation of embeddable potential sensor for corrosion monitoring in concrete structures

S. Muralidharan*, V. Saraswathy, A. Madhavamayandi, K. Thangavel, N. Palaniswamy

Corrosion Protection Division, Central Electrochemical Research Institute, Karaikudi 630006, Tamilnadu, India

ARTICLE INFO

Article history:
Received 8 February 2008
Received in revised form 26 March 2008
Accepted 21 April 2008
Available online 4 May 2008

Keywords:
Reinforcement corrosion
Corrosion monitoring
Embeddable sensor
Potential sensor

ABSTRACT

Embeddable potential sensor based on MnO_2 was assembled and characterised in concrete. The stability, reversibility, polarisability and impedance characteristics have been studied with respect to known reference. The corrosion performance of reinforced steel with respect to MnO_2 sensor was monitored by different electrochemical techniques. Reversibility of MnO_2 sensor indicated that difference of ±5 mV between the forward and reverse scan indicates the better reversibility characteristics in concrete. The rebar potentials (E_R) of steel with respect to MnO_2 are −315 and −525 mV for passive and active conditions of rebar in concrete. The corrosion current from potentiodynamic polarisation and R_{ct} from a.c. impedance technique clearly differentiated the behaviour of steel embedded in chloride contaminated concrete (active condition) from uncontaminated concrete (passive condition) with respect to MnO_2 sensor. All these studies revealed that corrosion monitoring of steel in concrete using embedded MnO_2 as a better potential sensor for steel in concrete. In addition it is easy to fabricate for amenable miniaturisation, varied configuration as demanded for corrosion monitoring in concrete structures.

1. Introduction

Half-cell (or reversible electrode) to exist, a dynamic reversible equilibrium must be established between different material phases at least one of which is a metal and another must be an electrolyte solution. Gaseous (e.g. hydrogen) or solid non-metallic phases (e.g. silver chloride) may also be involved [1–5]. The potential of the half-cell is dependent upon the chemical potentials of the reactions involved [6]. There is no known method for determining the absolute potentials of a single electrode. The only sound procedure would be to combine the electrode with an electrode of known potential and to measure the electrochemical potential of the resulting cell.

Conventionally $Cu/CuSO_4$ electrode can be placed easily on an external surface of concrete but it develops significant errors due to large resistant path between the steel and surface [7]. Saturated calomel electrode (SCE) is used for all the electrochemical measurements in laboratory but not suitable for as an embeddable use in concrete structure. Ag/AgCl is a successful reference electrode for all electrochemical measurements. But the problem associated with usage of Ag/AgCl electrode is reported [8–14]. Graphite has also performed satisfactorily in concrete, but this is not thermodynamically a true sensor [15]. Commercially available Ti rods activated with mixed metal oxides was reported as a sensor for concrete [16]. The electrochemistry of MnO_2 is long had been studied and also successful depolariser in alkaline power sources [17,18]. The MnO_2-montmorillonite composite mass has been investigated as an all solid internal reference for pH sensors [19]. Humidity sensing of MnO_2 and its calcination products was investigated [20]. The electrochemical behaviour of MnO_2 on a gold electrode has been studied [21].

In laboratory situations, it is relatively simple matter to establish the correct operation of reference electrode and the stability of the observed potentials. The properties of reference electrodes depend upon the presence of particular stable phases and concentrations of species of the junction forming the reference potential. It is a fact that particular reference electrode may have a well defined and stable potential in one application does not mean that it will behave ideally in all situations where chemical, physical and environmental properties may undergo continuous and rapid changes. Ideally reference potential data should refer to the standard hydro-

Abbreviations: OPC, ordinary Portland cement; E_{corr1}, corrosion potential (Forward scan); E_{corr2}, corrosion potential (Reverse scan); CE, cement extract; CPS, concrete pore solution; SCS, saturated calcium hydroxide solution; E_{corr}, corrosion potential; I_{corr}, corrosion current; $E_{1/2}$, half-cell potential; E_R, rebar potential; SCE, saturated calomel electrode; MnO_2, manganese-di-oxide; CSH, calcium silicate hydrate; R_{ct}, charge transfer resistance; C_{dl}, double layer capacitance; mV, milli volt; S0, system with 0% chloride; S1, system with 1% chloride; S2, system with 2% chloride; S3, system with 3% chloride.

* Corresponding author. Tel.: +91 4565 227550/59; fax: +91 4565 227779.
E-mail address: corrmurali@yahoo.com (S. Muralidharan).

0013-4686/$ – see front matter © 2008 Elsevier Ltd. All rights reserved.
doi:10.1016/j.electacta.2008.04.078

gen electrode which is the primary reference. But often secondary reference electrodes are used in situations where their potential with respect to the primary reference is unknown. In addition it is often the case that a pseudo reference electrode such as platinum is used as a reference, without any knowledge of how its potential relates to the primary reference.

Corrosion monitoring, the health check up of these structures is an essential survey required for maintaining the service life of these structures [22]. Rebar potential measurements using surface mounted reference electrodes are generally used to characterise the rebar as active or passive state as per ASTM C-876-1994 [23]. This technique has limitations which can be used only for atmospherically exposed concrete structures. Even for atmospherically exposed concrete, the high resistivity of concrete and higher cover thickness provides inconsistent results. Moreover, all the electrochemical measurements without IR compensation lead to an error. In order to eliminate these errors in corrosion monitoring in concrete structures, the present investigation deals with characterisation and evaluation of alkaline solid embeddable MnO_2 as a potential sensor for concrete.

2. Experimental

The experimental programme was divided into two parts. The first part deal with the characterisation of MnO_2 sensor embedded in concrete with respect to SCE. The properties studied were stability, reversibility, polarisability and impedance behaviour. The second part deals with to evaluate the corrosion performance of steel in concrete with respect to MnO_2 by various electrochemical techniques.

2.1. Materials used

2.1.1. Cement

Ordinary Portland cement (OPC) (equivalent to ASTM C150) was used throughout this investigation. The chemical composition (wt.%) of OPC is given in Table 1.

2.1.2. Fine aggregate

Local clean river sand (fineness modulus of medium sand equal to 2.6) conforming to grading zone III of IS: 383-1970 was used. The specific gravity of fine aggregate was 2.4. The water absorption of fine aggregate was 0.5%.

2.1.3. Coarse aggregate

Locally available well graded aggregate of normal size greater than 4.75 mm and less than 16 mm having a fineness modulus of 2.72 was used as coarse aggregate.

2.1.4. Solution preparation

Cement extracts: Ordinary Portland cement was sieved through 150 μm sieve and extract was prepared as follows. 100 g of the cement was mixed with 100 ml of distilled water and shaken vigorously using a microid flask mechanical shaker for about 1 h. The extracts were then collected by filtration.

Saturated calcium hydroxide solution: AR grade CaO was ignited for a long time to remove any carbonate present in the sample and then cooled. About 1.85 g of CaO was dissolved in distilled water to get a saturated calcium hydroxide solution.

Concrete pore solution: Synthetic concrete pore solution consisted of 7.4 g NaOH and 36.6 g KOH per litre of saturated calcium hydroxide solution.

Table 1
Chemical composition of OPC

Constituents	OPC (wt.%)
SiO_2	20–21
Al_2O_3	5.2–5.6
Fe_2O_3	4.4–4.8
CaO	62–63
MgO	0.5–0.7
SO_3	2.4–2.8
Loss on ignition (LOI)	1.5–2.5

2.1.5. Casting of concrete specimens

A designed mix of M20 was used. For characterisation work, cubical concrete specimen of size 15 cm × 15 cm × 15 cm were cast with MnO_2 sensor [24] embedded centrally into the concrete. For evaluation part thermomechanically treated (TMT) cylindrical rod of size 50 mm long and 12 mm diameter were also embedded very near to the MnO_2 sensor. In both cases, concrete specimens were cast with 0, 1, 2 and 3% chloride by weight of cement. During casting, the moulds were mechanically vibrated. After 24 h, all the specimens were cured for 28 days in distilled water. Systems studied are S0, S1, S2 and S3 represents concrete with 0, 1, 2 and 3% chloride, respectively. Concrete specimens were kept in the exposure yard for about 1 year which allows the steel to sufficiently corrode in the chloride contaminated concrete in order to understand the behaviour of MnO_2 sensor in both chloride contaminated (active state) and uncontaminated (passive) concretes.

2.2. Methods

2.2.1. Half-cell potential ($E_{1/2}$) for MnO_2 sensor and rebar potential (E_R) for steel in concrete

Half-cell potential ($E_{1/2}$) of MnO_2 sensor with respect to SCE and rebar potential (E_R) of steel with respect to MnO_2 was monitored for concrete specimens during curing period. Six numbers of sensors have been tested for each test to get reproducible results.

2.2.2. Reversibility of MnO_2 sensor in concrete

Cyclic polarisation studies for MnO_2 sensor was carried out using ACM instruments UK (Field machine) with a potential range of −20 to +20 mV from open circuit potential and with a sweep rate of 1 mV s^{-1}. Three required electrodes to complete the circuit were MnO_2 sensor embedded in concrete, cubical square sized stainless steel and surface mounted saturated calomel electrode. The test solutions used for contact between concrete and external reference electrode were saturated calcium hydroxide solution (SCS), concrete pore solution (CPS) and cement extract (CE). A time interval of 10–15 min was given for each system to attain a steady state. Experiments were conducted at room temperature (35 ± 1 °C) for two cycles [forward scan (E_{corr1}) and reverse scan (E_{corr2})]. The $E_{1/2}$, E_{corr1}, E_{corr2} values were derived for MnO_2 sensor in all the three solutions.

2.2.3. Potentiodynamic polarisation behaviour of MnO_2 sensor

Potentiodynamic polarisation studies for embedded MnO_2 sensor in concrete and reinforced steel were carried out using ACM Instruments UK (Field machine) with a potential range of −200 to +200 mV from open circuit potential and with a sweep rate of 1 mV s^{-1}. Both anodic and cathodic polarisation curves were recorded for all the systems studied.

2.2.4. A.c. impedance behaviour of MnO_2 sensor in concrete

Impedance measurements for embedded MnO_2 sensors were carried out using ACM Instruments UK (Field machine) with a fre-

Table 2
Reversibility behaviour for embedded MnO_2 sensor in concrete

Solution	System	$E_{1/2}$ (mV vs. SCE)	E_{corr1} (mV vs. SCE)	E_{corr2} (mV vs. SCE)	Difference between E_{corr1} and E_{corr2} (mV vs. SCE)
SCS	S0	209	208	202	4
	S1	206	206	206	0
	S2	203	204	207	3
	S3	202	201	204	3
CPS	S0	200	200	202	2
	S1	207	206	206	0
	S2	201	205	202	3
	S3	205	207	204	3
CE	S0	206	203	207	4
	S1	200	208	203	5
	S2	209	203	208	5
	S3	201	201	202	1

quency range of 30 kHz to 10 mHz. Nyquist plots were recorded for all the systems studied.

3. Results and discussion

3.1. Characterisation of MnO_2 sensor embedded in concrete

3.1.1. Half-cell potential measurements for MnO_2 sensor in concrete

The half-cell potential ($E_{1/2}$) measured for MnO_2 sensor embedded in concrete containing 0, 1, 2 and 3% chloride during curing period is given in Fig. 1. Initially the $E_{1/2}$ values were found to be +181, +185, +187 and +188 mV vs. SCE for S0, S1, S2 and S3, respectively. At the end of curing, the measured values were found to be +200, +205, +207, +209 mV vs. SCE. During curing period, a slight variation was observed among the $E_{1/2}$ values which is due to the continuous hydration of cement in concrete with considerable liberation of heat. On the other hand, at the end of curing, the $E_{1/2}$ values became steady irrespective of chloride contents in concrete. This is due to the formation of calcium silicate hydrate (CSH) gel (final hydration product) would expect to complete in 28 days. The half-cell potential of MnO_2 in concrete was assessed as +200 mV vs. SCE and assumed from MnO_2/Mn_2O_3 equilibrium potential.

3.1.2. Reversibility behaviour of MnO_2 sensor in concrete

The cyclic polarisation curve for MnO_2 sensor embedded in concrete containing 0% chloride and immersed in SCS is given in Fig. 2.

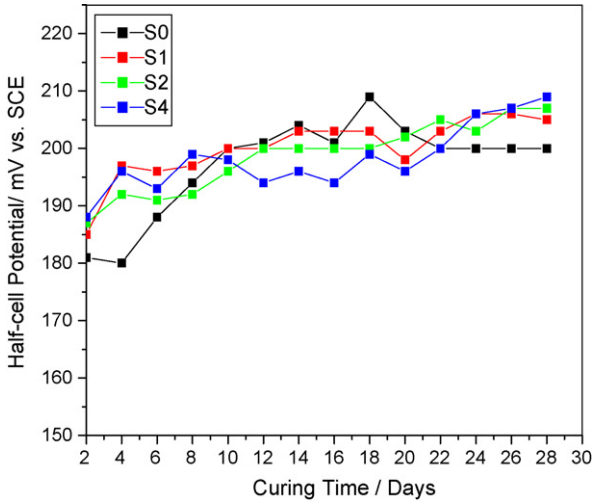

Fig. 1. Half-cell potential vs. curing time for MnO_2 sensor in concrete.

The $E_{1/2}$, E_{corr1} and E_{corr2} values derived for the different systems (S0–S3) are given in Table 2. The E_{corr1} and E_{corr2} values measured in each system were found to be almost close to the $E_{1/2}$ values. For example in SCS at 3% chloride contaminated concrete $E_{1/2}$, E_{corr1} and E_{corr2} values measured were +202, +201 and +204 mV, respectively. Similar observation was also observed in CPS and CE solutions. The difference between E_{corr1} and E_{corr2} was also found negligible. The maximum difference between forward and reverse scan is ±5 mV which indicated the better reversibility characteristics of MnO_2 sensor in concrete. The $E_{1/2}$ of MnO_2 sensor is not at all affected by the addition of various amounts of chloride in concrete. It indicates MnO_2 sensors exhibit their stability in concrete irrespective of chloride.

3.1.3. Polarisation behaviour of MnO_2 sensor in concrete

The potentiodynamic polarisation curve for MnO_2 sensor embedded in concrete containing 0% chloride and immersed in SCS is given in Fig. 3. The $E_{1/2}$, E_{corr} and I_{corr} values obtained for different systems (S0–S3) are reported in Table 3. The $E_{1/2}$ values at S0 was found to be +205, +200 and +200 mV vs. SCE in SCS, CPS and CE solutions, respectively. The E_{corr} obtained were also close to the $E_{1/2}$ values. For example in SCS system at 3% NaCl contaminated concrete, the $E_{1/2}$ and E_{corr} values measured were +202, +205 mV vs. SCE, respectively. Similar observation was also observed in CPS and CE solutions. The difference between $E_{1/2}$ and E_{corr} values measured for MnO_2 sensor in all the three solutions were found to be negligible. The I_{corr} values measured for MnO_2 sensor in the presence and absence of chloride contaminated concrete showed the same

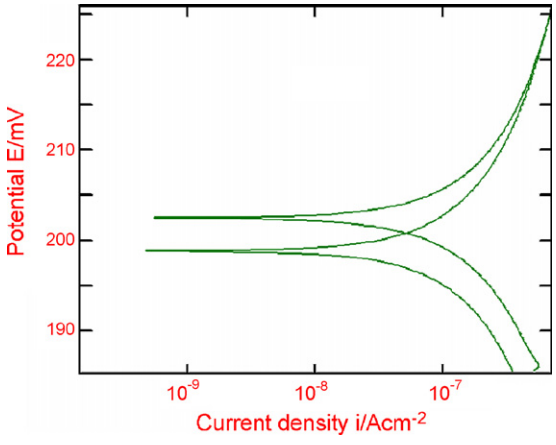

Fig. 2. Cyclic polarisation curve for MnO_2 sensor embedded in concrete containing 0% chloride and immersed in saturated calcium hydroxide solution.

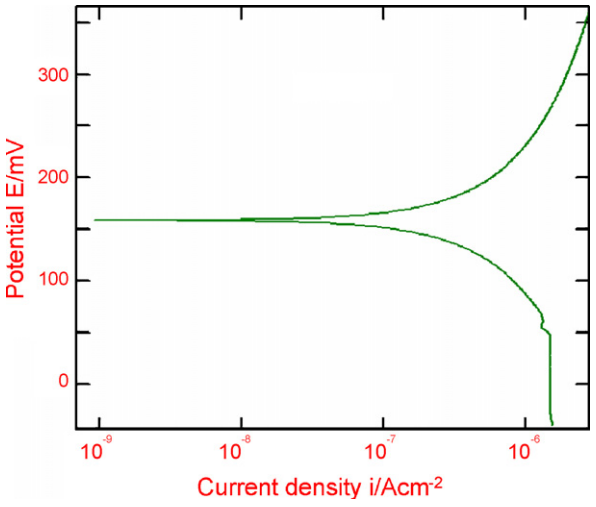

Fig. 3. Potentiodynamic polarisation curve for MnO_2 sensor embedded in concrete containing 0% chloride and immersed in saturated calcium hydroxide solution.

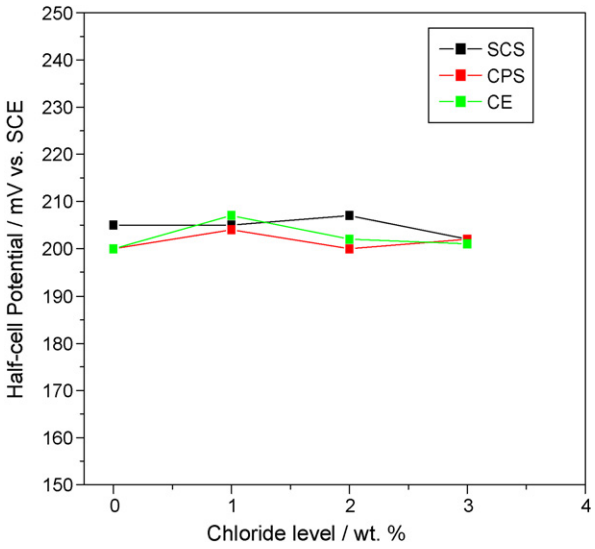

Fig. 4. Relation between half-cell potential and chloride level for MnO_2 sensor embedded in concrete.

order of magnitude of 10^{-5} in all the systems studied. The negligible difference in corrosion current measured in presence and absence of chloride indicated the perfect stability of MnO_2 sensor as an embeddable use in concrete. MnO_2 sensor showed very negligible corrosion current indicating the minimum polarisation of MnO_2 sensor in concrete environments. No significant change in the corrosion current and corrosion potential values in the presence of chloride. The relation between $E_{1/2}$ and chloride level is given in Fig. 4. The presence of chloride does not affect the performance of MnO_2 sensor in concrete. It is well known fact that steel in concrete usually in passive condition, but in the presence of corrosive ions it becomes active condition. It is necessary that sensor embedded in concrete to prevail in any conditions in order to maintain their stability. In that case MnO_2 sensor performed well in both the active and passive conditions.

3.1.4. A.c. impedance behaviour of MnO_2 sensor embedded in concrete

The impedance curve for MnO_2 sensor embedded in concrete containing 0% Cl^- and immersed in SCS are given in Fig. 5. The $E_{1/2}$, charge transfer resistance (R_{ct}) and double layer capacitance (C_{dl}) values obtained for different systems are given in Table 4. The $E_{1/2}$ values for MnO_2 in system S0 was +205, +200 and +204 mV vs. SCE in SCS, CPS and CE solutions respectively whereas that in system S3 was +204, +206 and +200 mV vs. SCE.

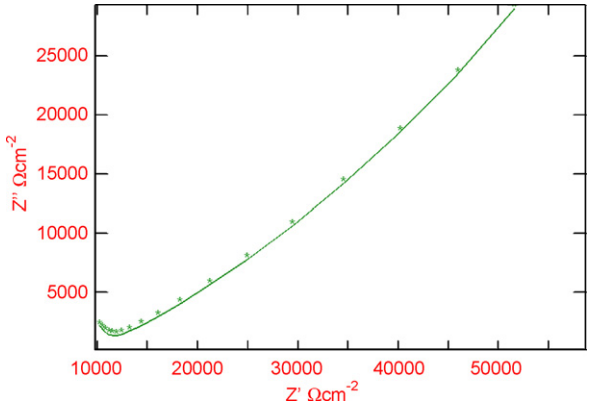

Fig. 5. Impedance plot for MnO_2 sensor embedded in concrete containing 0% chloride and immersed in saturated calcium hydroxide solution.

The R_{ct} values for MnO_2 sensor in system S0 was 2.010×10^4, 1.585×10^4 and $1.311 \times 10^4\ \Omega\,cm^2$ in SCS, CPS and CE solutions, respectively. There was not much variation observed in R_{ct} value for chloride contaminated concrete. From these data, the R_{ct} values measured for MnO_2 sensor in the presence and absence of chloride contaminated concrete showed the same order of magnitude of

Table 3
Polarisation parameters for embedded MnO_2 sensor in concrete

Solution	System	$E_{1/2}$ (mV vs. SCE)	E_{corr} (mV vs. SCE)	Tafel slopes (mV dec^{-1})		Icorr ($\times 10^{-5}$ mA cm^{-2})
				ba	*bc*	
SCS	S0	205	200	70	63	2.16
	S1	205	200	78	68	2.18
	S2	207	200	77	66	2.25
	S3	202	205	70	62	2.57
CPS	S0	200	200	74	65	2.39
	S1	204	202	70	61	2.53
	S2	200	201	74	68	2.53
	S3	202	205	70	60	2.95
CE	S0	200	200	74	62	2.41
	S1	207	202	74	65	2.77
	S2	202	200	76	65	2.78
	S3	201	200	73	63	2.78

Table 4
Impedance parameters for embedded MnO_2 sensor in concrete

Solution	System	$E_{1/2}$ (mV vs. SCE)	R_{ct} ($\times 10^4\ \Omega\,cm^2$)	C_{dl} ($\times 10^{-5}$ F cm^{-2})
SCS	S0	205	2.010	1.620
	S1	206	1.475	1.777
	S2	201	1.424	1.729
	S3	204	1.039	1.588
CPS	S0	200	1.585	1.996
	S1	201	1.432	1.440
	S2	206	1.099	1.078
	S3	206	0.937	1.537
CE	S0	204	1.311	1.189
	S1	208	1.260	1.949
	S2	202	1.248	1.010
	S3	200	0.867	1.355

$10^4\ \Omega\,cm^2$ in all the three solutions. The C_{dl} values are much lower than the R_{ct} values for all the system studied. No significant change in the C_{dl} values were observed between various systems. The negligible difference measured among $E_{1/2}$, R_{ct} and C_{dl} values in the presence and absence of chloride indicated the good performance of MnO_2 sensor in concrete. As observed earlier chloride have no influence on the performance of sensor in concrete.

3.2. Evaluation of MnO_2 sensor in concrete

3.2.1. Rebar potential measurements (E_R) of steel in concrete

Rebar potential (E_R) measured for steel in concrete containing 0, 1, 2 and 3% chloride with respect to MnO_2 during curing period is given in Fig. 6. Initially the rebar potentials were −310, −320, −332 and −345 mV vs. MnO_2 for S0, S1, S2 and S3, respectively. After 28 days of curing the measured values were −315, −322, −330 and −345 mV vs. MnO_2. Chloride contaminated system showed slightly negative OCP than control system. The galvanic coupling between the reference sensor and the embedded steel in concrete is a measure of the MnO_2/Mn_2O_3 equilibrium potential and Fe/Fe^{2+}.

3.2.2. Potentiodynamic polarisation of steel in concrete

The potentiodynamic polarisation curve for steel in concrete containing 0% chloride and immersed in SCS is given in Fig. 7. The E_R, E_{corr} and I_{corr} values obtained for different systems (S0–S3) in SCS, CPS and CE are reported in Table 5. The E_R values measured for steel in system S0 was −310, −313 and −315 mV vs. MnO_2 in SCS, CPS and CE solutions respectively, whereas in system S3 was −525, −535 and −536 mV vs. MnO_2 in SCS, CPS and CE solutions, respectively. These data showed that embedded steel in passive condition and active condition exhibited potential value of −312 and −532 mV vs. MnO_2, respectively.

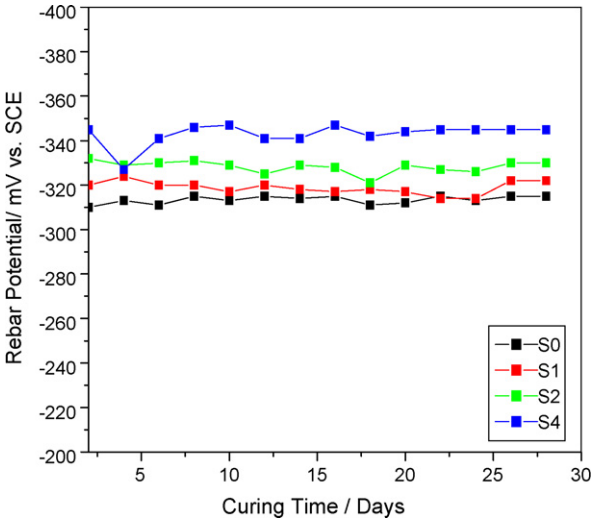

Fig. 6. Rebar potential vs. curing time for MnO_2 sensor in concrete.

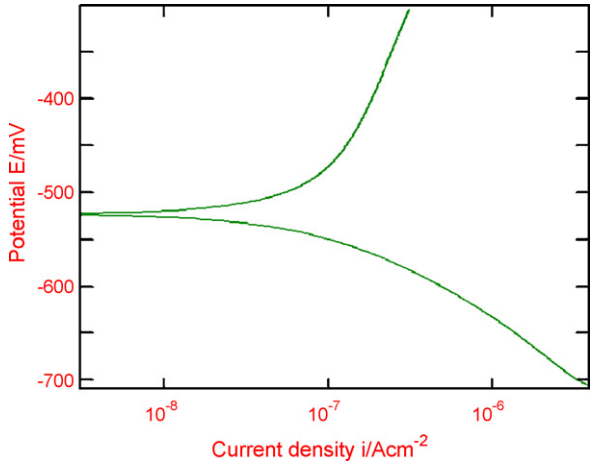

Fig. 7. Potentiodynamic polarisation curve for steel in concrete under passive condition (no chloride) and immersed in saturated calcium hydroxide solution.

The E_{corr} values measured for steel in system S0 was −325, −320 and −320 mV vs. MnO_2 in SCS, CPS and CE solutions, respectively. On the other hand in system S3 was −565, −560 and −570 mV in SCS, CPS and CE, respectively. These data clearly distinguished the behaviour of steel in active condition from passive conditions. The I_{corr} values measured for steel in system S0 was 3.04×10^{-5},

Table 5
Polarisation parameters for embedded steel in concrete

Solution	System	E_R (mV vs. MnO_2)	Tafel slopes (mV dec^{-1})		I_{corr} ($\times 10^{-5}$ mA cm^{-2})	E_{corr} (mV vs. MnO_2)
			ba	*bc*		
SCS	S0	−310	95	58	3.04	−325
	S1	−353	36	16	8.52	−355
	S2	−465	39	30	9.62	−500
	S3	−525	40	19	14.66	−565
CPS	S0	−313	97	50	2.77	−320
	S1	−355	34	21	8.25	−365
	S2	−462	39	30	9.25	−501
	S3	−535	46	28	13.25	−560
CE	S0	−315	98	57	3.27	−320
	S1	−352	44	34	8.85	−370
	S2	−467	36	25	9.63	−505
	S3	−536	42	27	15.28	−570

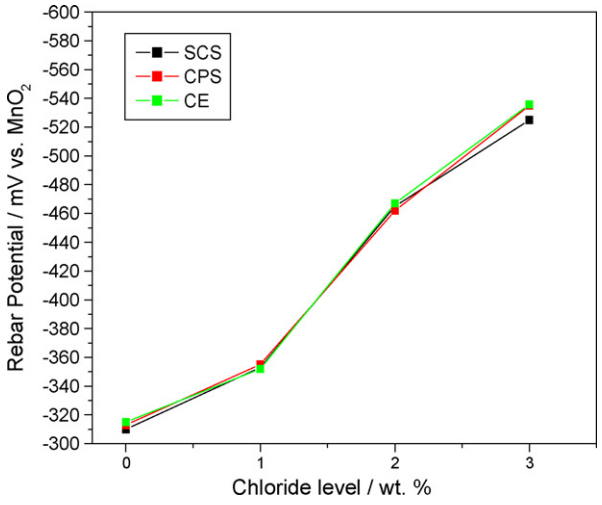

Fig. 8. Relation between rebar potential and chloride level for steel in concrete.

2.77×10^{-5} and 3.27×10^{-5} mA cm^{-2} in SCS, CPS and CE solutions respectively whereas that in chloride contaminated concrete were found to vary from 8.25×10^{-5} to 15.28×10^{-5} mA cm^{-2} depending on chloride contents.

The relation between E_R and chloride level for steel in concrete is given in Fig. 8. It was observed that the E_R of steel increases with increasing chloride level in concrete. These data also clearly distinguished the behaviour of steel in active condition from passive condition. Here it is pointed out that MnO_2 sensor able to distinguish the potential of steel either in active or passive conditions in concrete. This behaviour is quite suited for our interest to use the MnO_2 sensor in corrosion monitoring of steel in concrete.

3.2.3. *A.c. impedance studies on steel in concrete*

The impedance curve for steel embedded in concrete containing 0% chloride and immersed in SCS is given in Fig. 9. The impedance parameters for steel in concrete for different systems (S0–S3) in SCS, CPS and CE are given in Table 6. The E_R values measured for steel in system S0 was −315, −314 and −316 mV vs. MnO_2 in SCS, CPS and CE, respectively. But in the case of system S3 the values observed were −520, −525 and −530 mV in SCS, CPS and CE, respectively. These data showed that embedded steel in passive and

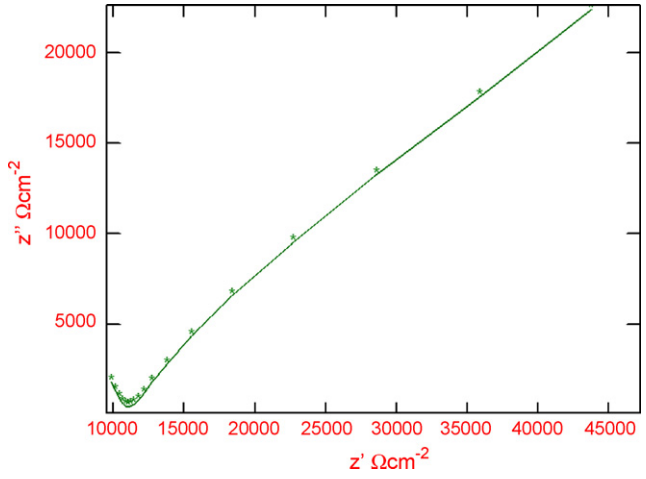

Fig. 9. Impedance plot for steel in concrete under passive condition (no chloride) and immersed in saturated calcium hydroxide solution.

Table 6
Impedance parameters for embedded steel in concrete

Solution	System	E_R (mV vs. MnO_2)	R_{ct} ($\times 10^4$ Ω cm^2)	C_{dl} ($\times 10^{-5}$ F cm^{-2})
SCS	S0	−315	2.010	1.620
	S1	−355	1.475	3.729
	S2	−460	1.424	3.777
	S3	−520	1.039	5.588
CPS	S0	−314	1.585	1.078
	S1	−358	1.432	3.440
	S2	−464	1.099	3.996
	S3	−525	0.937	5.375
CE	S0	−316	1.311	1.355
	S1	−357	1.260	3.890
	S2	−465	1.248	3.949
	S3	−530	0.867	6.010

active condition exhibited potential values of −315 and −525 mV vs. MnO_2, respectively. R_{ct} values measured for steel in system S0 was 2.010×10^4, 1.585×10^4 and 1.311×10^4 Ω cm^2 in SCS, CPS and CE solutions, respectively. But in the case of system S3 the values were 1.039×10^4, 0.937×10^4 and 0.867×10^4 Ω cm^2 respectively in SCS, CPS and CE solutions. These data clearly showed that higher R_{ct} values for steel in passive state and lower R_{ct} values for steel in active state. Similarly there is a definite trend obtained among C_{dl} values between active and passive state of steel in concrete.

4. Conclusions

The half-cell potential measurements indicated that $E_{1/2}$ of MnO_2 sensor in concrete is +200 mV vs. SCE. Reversibility of MnO_2 sensor indicated that difference between E_{corr1} and E_{corr2} is ±5 mV which is well within the limit as a better sensor for concrete. It indicates the better reversibility characteristics in concrete. The polarisation parameters for MnO_2 sensor showed negligible difference between half-cell potential $E_{1/2}$ and corrosion potential confirmed the stability of MnO_2 sensor in concrete. The impedance parameters further confirmed the perfect stability of sensor in concrete. The rebar potential of steel with respect to MnO_2 are −315 and −525 mV for passive and active conditions of rebar in concrete. The corrosion current from potentiodynamic polarisation and R_{ct} from impedance technique clearly differentiated the behaviour of steel whether in active or passive state with respect to MnO_2 sensor. All these studies revealed that corrosion monitoring of steel in concrete using embedded MnO_2 as a better potential sensor for steel in concrete. In addition it is easy to fabricate for amenable miniaturisation, varied configuration as demanded for corrosion monitoring in concrete structures.

Acknowledgement

The authors thank the Director, CECRI, Karaikudi for his kind permission to publish this paper.

References

[1] D.A. Eden, G.P. Quirk, Reference electrodes in plant corrosion monitoring who needs them, Corrosion, 2001, Paper No. 01303.
[2] L.A. Krebs, A brief history of corrosion sensing methods, Corrosion 2003, Paper No. 03419, p. 1.
[3] H. Suzuki, T. Hirakawa, S. Sasaki, I. Karube, Sens. Actuators B 46 (1998) 146.
[4] S. Itoh, F. Kobayashi, K. Baba, Y. Asano, H. Wada, Talanta 13 (1996) 135.
[5] M.A. Nolan, S.H. Tan, S.P. Kounaves, Anal. Chem. 69 (1997) 1244.
[6] A. Morz, M. Borchardt, C. Diekmann, K. Cammann, M. Knoll, C. Dumshat, Analyst 123 (1998) 1373.
[7] T.-H. Ha, S. Muralidharan, J.H. Bae, Y.C. Ha, H.G. Lee, K.W. Park, D.K. Kim, Sens. Mater. 16 (2004) 133.
[8] H. Suzuki, A. Hiratsuka, S. Sasaki, I. Karube, Sens. Actuators B 46 (1998) 104.
[9] H.C. Shell, D.G. Manning, Corrosion/85, NACE, Houston, TX, 1985, p. 263.

[10] J.E. Bennett, T.A. Mitchell, Corrosion/92, NACE, Houston, TX, 1992, p. 191.
[11] E. Lindner, Anal. Chem. 72 (2000) 336A.
[12] E. Bakker, Electroanalysis 11 (1999) 788.
[13] H.J. Lee, U.S. Hong, D.K. Lee, J.H. Shin, H. Nam, G.S. Cha, Anal. Chem. 70 (1998) 3377.
[14] M. Ciobanu, J.P. Wilburn, N.I. Buss, P. Ditavong, D.A. Lorry, Electroanalysis 14 (2002) 89.
[15] Use of reference electrodes for atmospherically exposed reinforced concrete structures, NACE Technical Committee Report 11100, March 2000.
[16] P. Castro, A.A. Sagues, E.I. Moreno, L. Maldonado, J. Genesca, Corrosion 52 (1996) 609.
[17] N.N. Greenwood, A. Earnshaw, Chemistry of Elements, 2nd ed., Butterworth-Heinemann, Oxford, 1997.
[18] D. Linden, Handbook of Batteries, McGraw-Hill, Maidenhead, 1995.
[19] L. Telli, B. Brahimi, A. Hammouche, Solid State Ionics 128 (2000) 255.
[20] C.-N. Xu, K. Miyazaki, T. Watanabe, Sens. Actuators B 46 (1998) 87.
[21] Z. Rogulski, H. Siwek, I. Paleska, A. Czerwinski, J. Electroanal. Chem. 543 (2003) 175.
[22] O. Klinhoffer, H. Arup, J. Mietz, Euro Corr 97, Trendheim, September, 1997.
[23] Annual book of ASTM standards (1994) C 876.
[24] S. Muralidharan, V. Saraswathy, K. Thangavel, N. Palaniswamy, Sens. Actuators B 130 (2008) 864.